Science of the Total Environment 873 (2023) 162175

Contents lists available at ScienceDirect

Science of the Total Environment

journal homepage: www.elsevier.com/locate/scitotenv

Land use change increases contaminant sequestration in blue carbon sediments

Stephen R. Conrad [a], Isaac R. Santos [a,b], Shane A. White [a], Ceylena J. Holloway [a], Dylan R. Brown [a], Praktan D. Wadnerkar [a], Rogger E. Correa [a,c], Rebecca L. Woodrow [a], Christian J. Sanders [a,*]

[a] National Marine Science Centre, School of Environment, Science and Engineering, Southern Cross University, P.O. Box 157, Coffs Harbour, NSW 2540, Australia
[b] Department of Marine Sciences, University of Gothenburg, P.O. Box 461, 40530 Gothenburg, Sweden
[c] Corporacion Merceditas – Merceditas Corporation, Medellín, Colombia

HIGHLIGHTS

- Twenty-five ^{210}Pb dated sediment cores were examined for contaminant accumulation.
- Contaminants (trace metal, metalloid, and P) in soils increase with development.
- >30 % development resulted in a 20 to 350 % increase in P, Cd, Zn, Pb, Mn and As accumulation.
- Our results demonstrate the capacity of blue carbon habitats to sequester contaminants.

GRAPHICAL ABSTRACT

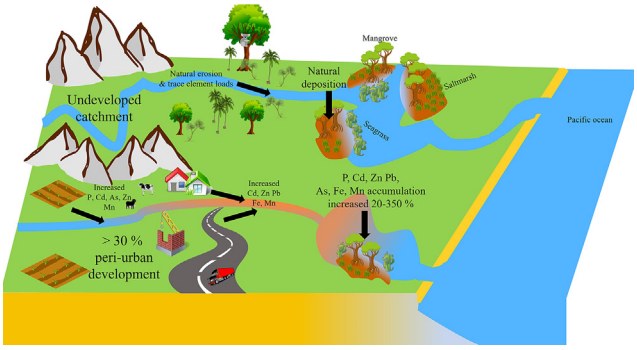

ARTICLE INFO

Editor: Julian Blasco

Keywords:
Mangrove
Saltmarsh
Seagrass
Trace metal
Metalloid
Phosphorus

ABSTRACT

Coastal blue carbon habitats perform many important environmental functions, including long-term carbon and anthropogenic contaminant storage. Here, we analysed twenty-five ^{210}Pb-dated mangrove, saltmarsh, and seagrass sediment cores from six estuaries across a land-use gradient to determine metal, metalloid, and phosphorous sedimentary fluxes. Cadmium, arsenic, iron, and manganese had linear to exponential positive correlations between concentrations, sediment flux, geoaccumulation index, and catchment development. Increases in anthropogenic development (agricultural or urban land uses) from >30 % of the total catchment area enhanced mean concentrations of arsenic, copper, iron, manganese, and zinc between 1.5 and 4.3-fold. A ~ 30 % anthropogenic land-use was the threshold in which blue carbon sediment quality begins to be detrimentally impacted on an entire estuary scale. Fluxes of phosphorous, cadmium, lead, and aluminium responded similarly, increasing 1.2 to 2.5-fold when anthropogenic land-use increased by at least 5 %. Exponential increases in phosphorus flux to estuary sediments seem to precede eutrophication as observed in more developed estuaries. Overall, multiple lines of evidence revealed how catchment development drives blue carbon sediment quality across a regional scale.

1. Introduction

Seagrass, saltmarsh, and mangrove habitats play an important role in the global marine carbon (C) cycle (Lovelock and Duarte, 2019). While much of the literature has focused on C sequestration in blue carbon sediments (Macreadie et al., 2019; Wang et al., 2021b), their ability to improve

* Corresponding author.
E-mail address: christian.sanders@scu.edu.au (C.J. Sanders).

http://dx.doi.org/10.1016/j.scitotenv.2023.162175
Received 9 October 2022; Received in revised form 24 January 2023; Accepted 7 February 2023
Available online 17 February 2023

estuarine water quality via contaminant removal is also a valuable ecosystem service (Teuchies et al., 2013; Lee et al., 2019; Wadnerkar et al., 2019). Sediments of blue carbon habitats bury anthropogenic contaminants, such as phosphorous, trace metals, and metalloids (Williams et al., 1994; Nicolaidou and Nott, 1998; Conrad et al., 2019b) along with carbon, preventing terrestrially derived pollutants from reaching ecologically and commercially important coastal waters (Alongi and McKinnon, 2005). Catchment urbanisation and agriculture can accelerate the accumulation of contaminants in coastal sediments (Brush, 1989). Development disturbs soils by leaching contaminants from fertilizers, industrial, and natural sources (Walling, 1999; Das et al., 2009), which eventually reach estuaries (Conrad et al., 2019b; Conrad et al., 2020). Due to their low-lying topography and ability to accumulate sediments in pace with relative sea level rise, blue carbon habitats consistently receive and accrete sediments (Mcleod et al., 2011) which can reflect the development in the adjacent terrestrial environment (Machado et al., 2016; Conrad et al., 2017).

Several techniques have been used to resolve contaminant history in blue carbon sediments. Radionuclide dating, such as with ^{210}Pb, is a valuable tool to date sediments and link sedimentary profiles to historical anthropogenic development (Valette-Silver, 1993). By comparing nutrient and trace metal/metalloid concentrations in sediments dated before development, the deviation from pre-industrial sediment quality can be assessed (Sanders et al., 2014; Machado et al., 2016). Other metrics, like the geoaccumulation index (I_{geo}), are often-used to assess the difference between recent sediments from their previous natural (background) state (Muller, 1969; Liu et al., 2011; Chaudhary et al., 2013). Multivariate statistical methods, such as principal component analysis (PCA), can then be used to determine the specific impacts of different land uses on sediment quality (Vaalgamaa and Conley, 2008; Duodu et al., 2017). Combined, these geochronological and statistical analyses may reveal the role blue carbon sediments have in retaining anthropogenic contaminants across temporal, spatial, and land use gradients.

Here, we hypothesize that increasing catchment development will accelerate the burial of contaminants in blue carbon habitats. We rely on ^{210}Pb dated sediment cores from mangrove, saltmarsh, and seagrass habitats across a land use gradient in six estuaries. To resolve linkages and thresholds in catchment development resulting in a response in sediment quality, we measured contaminant concentrations, flux rates, and geoaccumulation indices. Our study identifies the extent to which anthropogenic development influences contaminant burial in blue carbon ecosystems.

2. Materials and methods

2.1. Study area

This study was undertaken in six estuaries with similar geomorphology and climate, spanning ~140 km along the subtropical New South Wales (NSW) north coast (Fig. 1). All estuaries contained *Avicennia marina* mangrove, *Sporobolus virginicus* and *Juncus krausii* saltmarsh, and *Zostera marina* seagrass vegetation with organic-rich sandy to fine-grained sediments (Conrad et al., 2019a). In this region of Australia, strong episodic rainfall promotes the mobilisation of contaminants into estuaries (Eyre, 1998; Conrad et al., 2020), with estuary sediments retaining contamination histories (Conrad et al., 2017; Conrad et al., 2019b). The upstream catchments contain mostly podzol, ferrosol, and humic clay soils. Land use varies in each catchment from peri-urban residential and agricultural (Boambee and Coffs), intense horticulture and large-scale livestock grazing (Hearnes and Clarence), to a high degree of land conservation with undisturbed National Park and native vegetation (Corindi and Wooli) (Fig. 1). Coffs, Hearnes, Corindi, and Wooli estuaries hydraulically connect with an area of biodiversity and commercial importance, the state-protected Solitary Islands Marine Park.

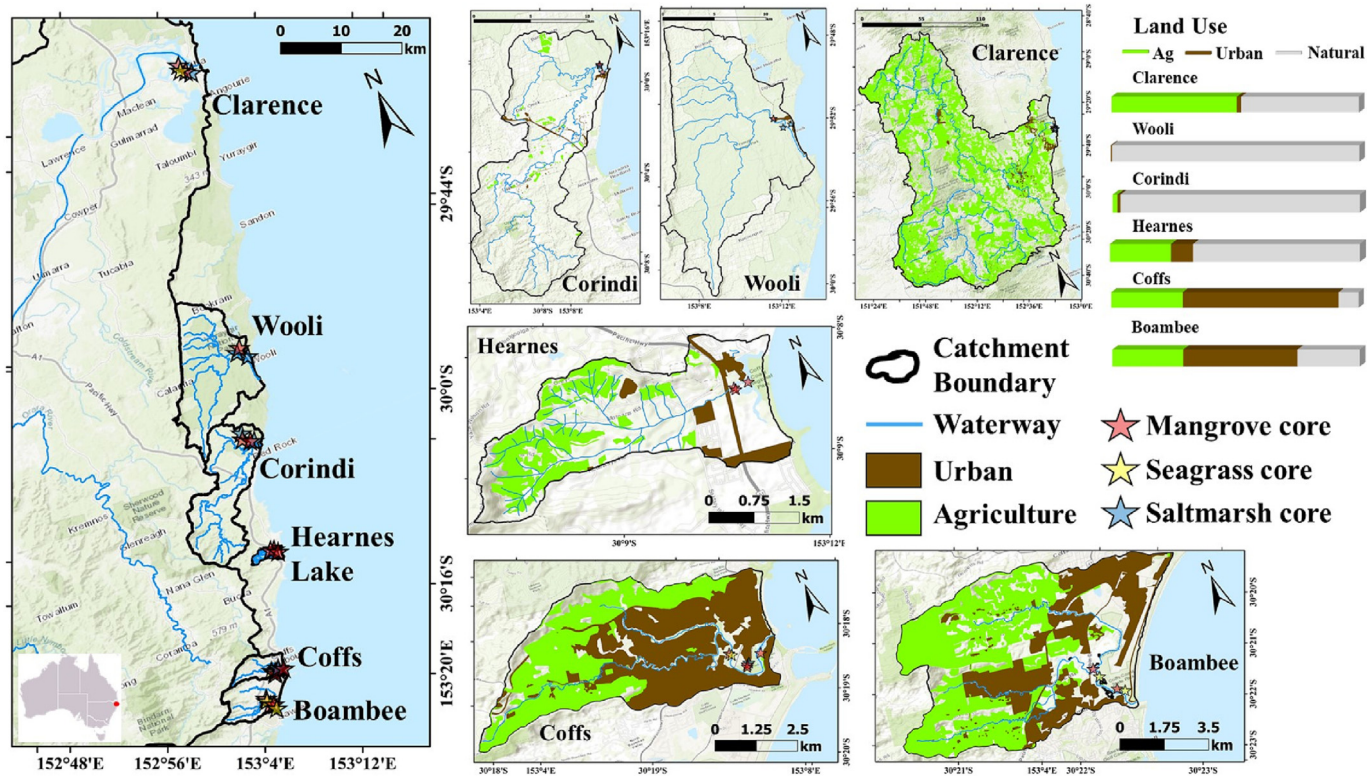

Fig. 1. Location, land use, and sample sites (stars) for and mangrove, seagrass, and saltmarsh sediment cores (n = 16, 4, and 5, respectively) of 6 estuary catchments on the subtropical coast of Eastern Australia. Agricultural land use is green. Urban land use is brown. Catchments range from conserved (Corindi, Wooli) to heavily developed (Boambee, Coffs).

Table 1
Sediment core sample coordinates (decimal degrees) and type (M = mangrove core, SM = saltmarsh core, SG = seagrass core).

Estuary	Cores	Core ID	Lat.	Long.
	M, SM, SG		Decimal °	
Clarence	2, 1, 1	M1	−29.41837	153.32988
		M3	−29.42176	153.33186
		SM3	−29.42096	153.33060
		SG3	−29.42194	153.33136
Wooli	2, 1, 0	M2	−29.859730	153.255659
		SM3	−29.860057	153.265607
		M4	−29.848819	153.253448
Corindi	2, 1,1	M1	−29.980404	153.225302
		SM1	−29.980404	153.225034
		M2	−29.975674	153.222179
		SM2	−29.976269	153.221941
Hearnes	3, 0, 0	M1	−30.123888	153.195873
		M2	−30.123600	153.195862
		M3	−30.123471	153.197855
Coffs	4, 1, 1	M1	−30.298783	153.124431
		M2L	−30.298911	153.124808
		M2H	−30.303394	153.129606
		SG2	−30.303631	153.129383
		M3	−30.303875	153.129156
		SM3	−30.301008	153.133953
Boambee	3, 0, 2	SG2	−30.349720	153.100035
		M3U	−30.347940	153.097810
		M3L	−30.347730	153.098340
		SG6	−30.339679	153.097092
		M7	−30.336820	153.093830

2.2. Sample collection and metal, metalloid, and phosphorous determination

We collected 25 sediment cores (16 mangrove, 5 saltmarsh, and 4 seagrass) from six sites across a land use gradient (Fig. 1, Table 1) using a 50-cm long, 5-cm diameter Russian peat auger or 6.7-mm inner-diameter PVC pipes. Peat auger cores were sectioned into 2 cm intervals upon return to the lab. Cores taken in the PVC pipe were extruded from the top of the tube and sectioned into 2 cm intervals in the field. Compaction was accounted for in core depth measurements on-site (Morton and White, 1997).

Metal, metalloid (As, Cu, Pb, Cd, Zn, Cr, Hg, Fe, Al), and phosphorus (P) contents were measured in each sediment interval. The total quantity of sediment intervals analyzed were based on the age, up to 100 years, of which may vary between sites. To extract contaminants from sediments, we used a one hour 1:3 HNO3/HCl hotplate (120 °C) acid digestion (Sastre et al., 2002). The extract was analysed on a Perkin Elmer NexlON 350D inductively coupled plasma mass spectrometer (ICP-MS) using American Public Health Association (APHA) 3125 In-House S6 methodology (Garbarino et al., 2006). Kinetic energy discrimination (KED) mode was used to remove interferences (Yamada, 2015). The ICP-MS was calibrated using standard curves ($R^2 \geq 0.999$) from certified stock solutions diluted to working concentrations. To confirm accuracy and precision of the instrument, sediment reference materials were digested (AGAL 12) with each sample batch. Instrument drift was routinely monitored by re-analysing our mid-point calibrations every 20 samples using internal Sc, Ge, Rh, and Ir standards. Recovery ranged between 85 and 105 %. Raw results were corrected based on independent calibration verification standards. Raw instrument data was calculated using by dividing the final digest volume (25 mL) by the sample weight used in the digest, then multiplying by ten to account for dilution pre-analysis (i.e., 25/sample weight) *10)), yielding a mass per mass result (i.e. mg kg^{-1}). All concentration data are available in the supporting information.

2.3. ^{210}Pb analysis and dating

^{210}Pb and ^{226}Ra gamma emission activities from core samples were counted in Canberra High Purity Germanium (HPGe) gamma detectors. Each sample was counted until the ^{210}Pb counting errors were < 10 %, following the protocols outlined in Brown et al., 2019 (Brown et al., 2019). Samples were packed into 99.34 cm^3 plastic petri dishes (30 to 115 g of sediment for broad energy detectors) or 13 mm diameter plastic vials to a height of 27 mm (14.3 cm^{-3}, 2 to 8 g of sediment, well detectors). To obtain sufficient sample mass, we combined two 2-cm sediment intervals from Wooli, Corindi, Coffs, and Boambee cores. Sediment from these adjacent intervals was combined immediately after homogenisation. The combined sample was physically agitated before being packed into the vials. All samples were sealed with PVC electrical tape (petri dish) or epoxy resin (vials) for at least 21 days to establish secular equilibrium between ^{222}Rn and its granddaughter ^{214}Pb. ^{210}Pb and ^{226}Ra decay was counted from the 46.5 keV and 295,2, 351.9, and 609.3 keV gamma peaks, respectively. Radionuclide counts per minute were multiplied by a correction factor that integrates background gamma ray intensity and detector efficiency determined from standard (USGS Rocky Flats) calibrations. Unsupported (or excess) ^{210}Pb ($^{210}Pb_{xs}$) was calculated by taking the difference of ^{210}Pb and ^{226}Ra activities for each dated sediment interval. Radionuclide counts from samples analysed in broad energy Ge detectors were corrected for self-absorption (Cutshall et al., 1983) before sedimentation rates were calculated. The vial samples did not require self-absorption due to the all-encompassing surface area provided by the cylindrical geometry of the well detector.

We calculated sediment ages using the constant initial concentration (CIC) model due to limited sample mass for radionuclide counting in some sediment intervals and occasionally insufficient sampling depth to reach the ^{210}Pb and ^{226}Ra equilibrium horizon. While the CIC model does not account for potential changes in sedimentation after anthropogenic development, it enables spatial comparisons of sedimentation and contaminant fluxes across a land use gradient. Furthermore, as sediment cores were taken within vegetated habitats, sedimentation rates would not be expected to change significantly as may be expected in bare sediments, such as mudflats (Wang et al., 2021b).

The CIC model generates an average rate of sediment accumulation down the entire core. Sedimentation rate was calculated:

$$C_m = C_0 \cdot e^{-\lambda t}$$

Where C_0 is initial excess ^{210}Pb activity, C_m is activity at depth, and λ is the ^{210}Pb decay constant (0.031) at sediment age t (Robbins and Edgington, 1975).

Sediment ages were calculated as:

$$\text{interval age} = \text{Year of collection} - \frac{\text{average interval depth}}{\text{sediment accumulation rate}}$$

When surface mixing was evident in sediment radionuclide profiles, these surface mixing layers were excluded (Arias-Ortiz et al., 2018). While all data from Boambee, Corindi, Wooli, Clarence, and 5 of the 6 Coffs cores are specific to this study, the ^{210}Pb data from Hearnes Lake and 1 Coffs mangrove core were originally reported elsewhere (Conrad et al., 2017; Conrad et al., 2019b).

To estimate contaminant fluxes to the sediment we first calculated sediment dry bulk density (DBD) by drying sediments at 40 °C until complete desiccation. The dry mass was divided by the wet sediment sample volume to obtain DBD. Finally, flux was calculated as

$$Flux = SAR * DBD * [Conc_x]$$

Where SAR = mean sediment accumulation rate for the core, as determined by the CIC dating model, DBD is dry bulk density, and $[Conc_x]$ is sediment concentration of contaminant x. Flux product is reported as mass of contaminant per area of mangrove sediments per unit time (ex: μg m^{-2} yr^{-1}) (Sanders et al., 2014).

2.4. Data analysis

Geoaccumulation index (I_{geo}) was calculated to assess the extent of pollution in the sediment cores (Muller, 1969). Geoaccumulation index was calculated for each contaminant using the equation:

$$I_{geo} = \log_2\left(\frac{C_n}{1.5B_n}\right)$$

where C_n is the measured contaminant content in sample n and B_n is the background concentration from n's sample location. The factor of 1.5 is introduced to compensate for variability in background concentrations due to natural lithogenic fluctuations. There are 7 classes of pollution in the geoaccumulation index: Class 0 ($I_{geo} \leq 0$, unpolluted) ranging to Class 6 ($I_{geo} > 5$ = severely polluted). To assess geological background values at the most local scale, contaminant contents from the bottom interval of each sediment core were used as background values for all calculations.

Delineations for each catchment were obtained from government databases (DPIE, 2019) and confirmed flow path tools in ESRI ArcMap v 10.5.1 on the upper limits of 1 m interval contour layers (ELVIS, 2021). Land use data was obtained from NSW DATABASE and modified by-hand by creating polygon shapefile layers from satellite imagery in ArcMap v. 10.5.1 (based on December 2018 imagery). We quantified land use in 3 categories: *Urban*- roads, communication infrastructure, commerce, manufacturing, industrial, mining, and residential areas (including rural residential, houses, apartments, lawns, parks); *Agricultural*- grazing, horticulture, farm infrastructure, production forestry, animal husbandry, and abandoned horticultural land that remained cleared and had no current urban use; and *Conserved*- undisturbed land cover with native vegetation, protected and maintained land (residential and/or national park, municipal nature reserve, state and/or national forest), and wetlands. Waterways were not considered in land use cover calculations.

Principal components analysis (PCA) was performed in XLSTAT (v 2021.1) software to reveal complex correlations between multiple contaminant concentrations, land use percentages, and estuary/catchment areas. Contaminant concentrations (in mg kg^{-1}) and sedimentation rate (cm yr^{-1}) data were found to be normally distributed after Box-Cox transformation (Zhang, 2006) and used as explanatory variables. Land use percentages (agricultural, urban, and conserved), estuary size (km^2), and catchment to estuary ratios (catchment km^2: estuary km^2) were entered as supplementary variables to observe how different land use categories correlate with contaminant concentrations in the PCA space. Best fit lines were calculated for land use with mean contaminant concentrations, fluxes, and I_{geo} using regression analysis.

We initially conducted all analyses with land uses (agriculture or urban) categorised separately, however there was a lack of distinct effects between specific land uses, as evident by the lack of correlation between sediment contaminant concentrations and agricultural or urban land use individually. Since peri-urban land use (rural/urban clash) is prominent throughout the region we combined cumulative agricultural and urban land uses. A clear trend of contamination across estuaries when cumulative total anthropogenic land use (agricultural + urban) was compared to sediment contaminant concentrations. Therefore, we combined agricultural and urban land uses, and hereby refer to this combination as 'developed' land use for further analyses.

3. Results and discussion

3.1. Land use and sedimentation rates

Land uses in each catchment ranged from highly conserved (Table 2) (Corindi and Wooli: > 85 % conserved land) to highly developed (Coffs, Boambee, and Clarence: 50 to 90 % agriculture and/or urban land use).

All cores displayed exponential decay of $^{210}Pb_{xs}$ (Fig. 2). Sedimentation rates ranged from 0.03 to 1.54 cm yr^{-1} (mean of 0.46 ± 0.10 cm yr^{-1}).The mean and upper limit of our estimated sedimentation rates are high compared to the literature, however within the range of sedimentation rates from other blue carbon systems reported (Miyajima et al., 2015; Sasmito et al., 2016; Woodroffe et al., 2016; Wang et al., 2021a). Year to depth models (Fig. 2) revealed that some bottom sediments date from beyond the range of ^{210}Pb dating (Corindi saltmarsh, 19 cm depth, year <1900) to 1990s (Boambee M3L and SG6 cores).

There was possible sedimentation rate variability along certain cores, as evidenced by deviations from the best fit line in $^{210}Pb_{xs}$ profiles (Fig. 2). Therefore, the intervals that deviate from the best fit line may not be representative of the overall mean sedimentation rate estimates and subsequent flux calculations should be interpreted with caution. However, the CIC dating method allowed for direct comparisons between cores and estuaries. There was also high variability in sedimentation rates across cores and habitats within each estuary as expected for estuarine sedimentary environments (McCave, 1984). Mean sedimentation rates in each estuary displayed no clear trend with land use percentages (R^2 = 0.06). Boambee cores had mean elevated sedimentation rates (0.95 ± 0.22 cm yr^{-1}) compared to the other cores (0.36 ± 0.02 cm yr^{-1}).

3.2. Concentrations, fluxes, and geoaccumulation indices

For most metal and metalloids, the estuaries with more combined urban and agriculture land uses (Coffs or Boambee) had the greatest mean concentrations. Mean As, Mn, and Fe concentrations were greatest in Boambee sediment cores, while Coffs Creek had the most highly elevated trace metal concentrations (Pb, Cd, and Zn) typically reflective of industrial or agricultural activities. The elevated mean concentrations of these trace elements in blue carbon sediments likely reflect the high degree of anthropogenic development in these estuaries (>70 % of land cover).

Although the blue carbon sediments of the further developed estuaries were generally more concentrated with trace and major metals/metalloids, there were several occurrences of isolated pollution within the less developed estuaries. Several sediment cores contained stray layers of contamination. For example, Corindi SM2 core had anomalously high concentrations of Al, As, Cu, P, and Zn at 29 cm depth, while Clarence SM3 had spikes of Al, As, Cr, Cu, Fe, Hg, and Zn at 9 cm depth. These layers are likely contaminated to high concentrations of trace elements due to redox-driven migration throughout the sediment column, including pyritization (Andrade et al., 2012). Spikes in these layers drove the Clarence and Corindi estuaries to have the greatest Cr and P concentrations, respectively. These layers of metal-rich sediment demonstrate how geochemical processes may distort interpretations of blue carbon sediment quality from localised (core) to catchment-scales.

Concentrations of Cd, Zn, Pb, Cu, and Fe increased exponentially, and Mn increased linearly with developed land use (Fig. 3). A similar relationship was observed for P, with the exception of the Corindi estuary, driven by the peculiarly polluted Corindi SM2 core (see concentration data for individual cores in Fig. 3). Catchment land use cover >30 % resulted in concentration increases between 1.5 and 4.25-fold for Zn, As, Cu, Fe, and Mn. This result suggests a catchment land use threshold of ~30 % development

Table 2
Characteristics and land use (Ag = agricultural) of six estuaries sampled in this study. Predominant impact was determined by the percentage and proximity of land uses in the upstream catchment.

Estuary	Catchment area	Estuary area	Catchment to estuary ratio	M	SM	SG	Conserved	Ag	Urban	Total developed	Predominant impact
	km^2	km^2		ha	ha	ha	%	%	%	%	
Clarence	22,716.00	0.02	1.10E+06	521	195	1907	45.2	50.7	1.7	52.4	Ag
Wooli	184	3.7	49.7	86	66.9	9.4	98	0	0.5	0.5	None
Corindi	148	1.9	77.9	37.1	52.7	2.4	85	1.9	1.2	3.4	None
Hearnes	6.8	0.1	68	6.1	3.2	0.1	24.8	24.4	8.8	33.2	Ag
Coffs	24.5	0.5	49	20.1	1.4	0.2	8	28.4	62.1	90.5	Urban
Boambee	48.5	1	48.5	33.1	2.9	6	24	28.6	46.2	74.8	Urban

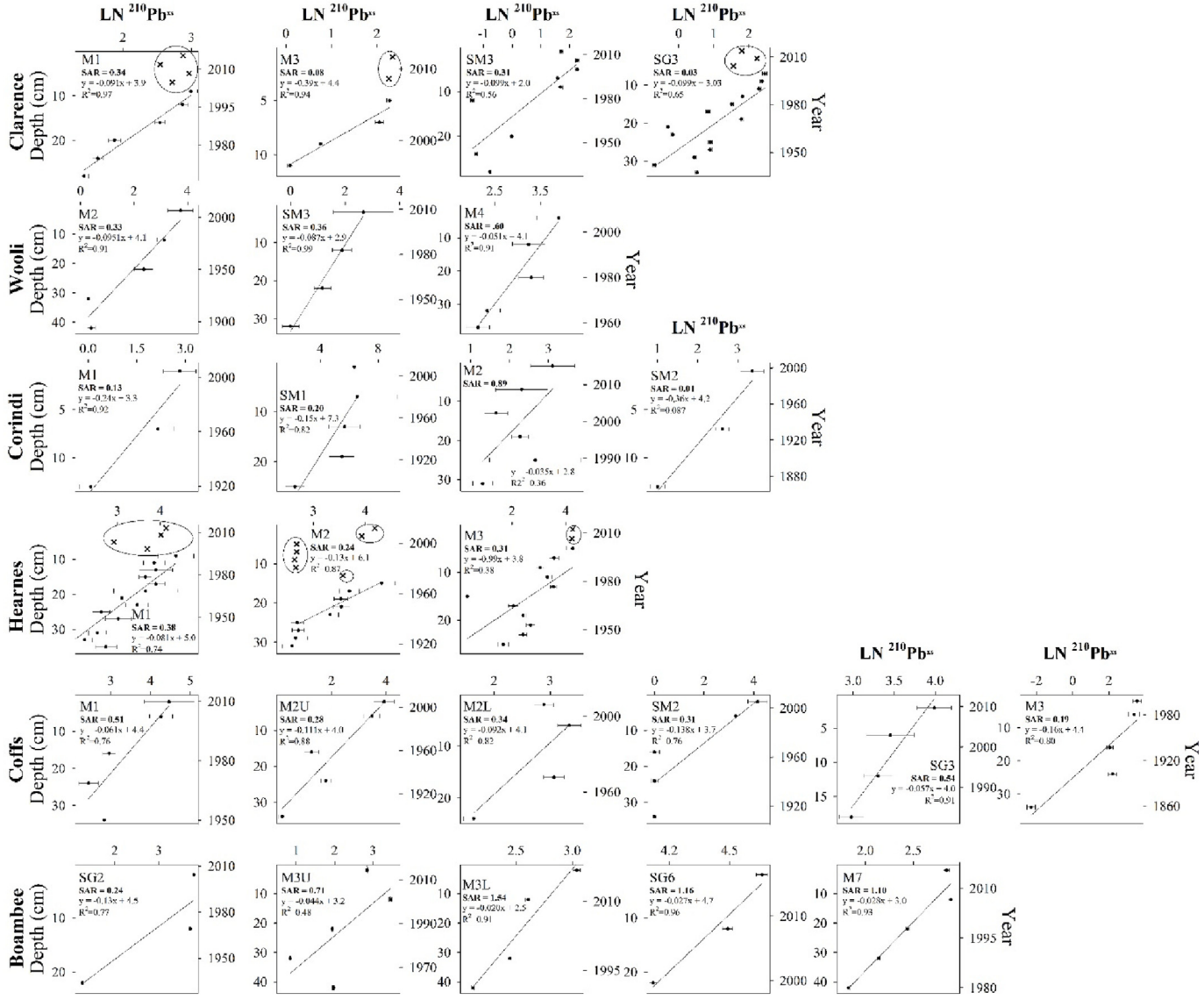

Fig. 2. Natural-log of excess ^{210}Pb (LN $^{210}Pb_{xs}$) decay and year-to-depth profiles from 25 sediment cores. Circled 'X' data points in Clarence and Hearnes cores represent surface mixing layer observations excluded from constant initial concentration dating model calculations. Error bars represent propagated $^{210}Pb_{xs}$ error (Harvard, 2007). M = mangrove core; SM = saltmarsh core; SG = seagrass core. Please note different scales of each axis for each core.

after which blue carbon sediment contaminant concentrations increase significantly.

Chromium, Hg, and Al concentrations lacked any apparent relationship with development (Fig. 3). This region lacks a major manufacturing industry and sources of Hg and Cr. The lack of relationship between development and Hg is probably due to relatively uniform atmospheric deposition across this region (Nelson et al., 2012). The anomalous Cr and Hg pollution observed within and across estuaries may reflect the great localised variability in metal, metalloid, and nutrient deposition and diagenesis within these constantly evolving blue carbon sedimentary environments (Spencer, 2002). Overall, sediment contaminant concentrations were lower than sediments of more developed estuaries in major metropolitan areas in Australia (Mackey and Hodgkinson, 1995; Irvine and Birch, 1998; Rate et al., 2000).

Despite no direct relations between development and sedimentation rates, the influence of development on contaminant flux was clear. Abundant lithogenic metals (Fe, Al, Mn) displayed positive correlations between fluxes and catchment development (Fig. 3), likely reflective of greater deposition of terrestrially-derived minerals (Fernandes and Nayak, 2020). Dissolved fractions of Cd, Zn, and Pb probably bind with these lithogenic metals during aquatic transport (Sholkovitz, 1978; Wen et al., 2008). Cd, Zn, and Pb may be introduced from roads, agriculture, and industrial activities (Alloway, 2013). While P concentrations and I_{geo} varied across the land use gradient, P fluxes had an exponential increase with development (Fig. 3). The negative trend of P I_{geo} may be driven by recent relatively large deviations from background P concentrations in more pristine sediments of less disturbed catchments. As development continues to expand in this region, increasing P fluxes may be antecedent to eutrophication that has persisted in more impacted subtropical Australian estuaries (Hodgkin and Hamilton, 1993; Davis and Koop, 2006). These fluxes of P, Cd, Zn, Pb, Cu, Hg are relatively low compared to areas with a higher population density or more intense industrial activities where fluxes of these elements were orders of magnitude greater (Ip et al., 2004; Sanders et al., 2006; de Carvalho Gomes et al., 2009; Baptista Neto et al., 2013; Sanders et al., 2014; Álvarez-Vázquez et al., 2017).

Mean I_{geo} values for most elements across all estuaries were negative or near 0 (Fig. 3), indicating minimal sediment pollution. The one exception to this trend was the severe contamination of Hg observed in the Clarence sediments (mean $I_{geo} > 4$, Fig. 3) related to the extremely low contents of Hg (< 1 ng kg^{-1}) at the bottom of the Clarence M3 core. Indeed, the relatively low

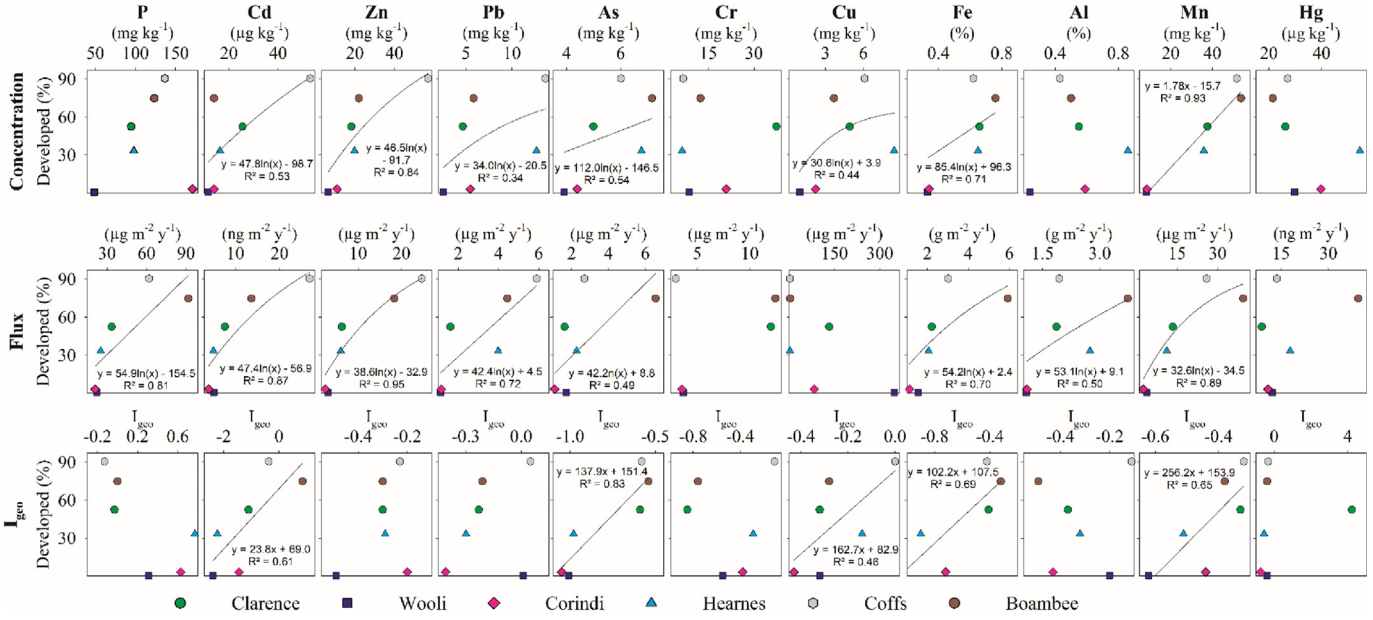

Fig. 3. Mean concentrations, fluxes, and geoaccumulation indices (I_{geo}) of metals, metalloids, and phosphorus from sediment cores compared to developed land use percentage from six estuaries. All habitat types (mangrove, saltmarsh, and seagrass) were averaged together here to obtain means for all sediment cores within each estuary. Lines of best fit (linear or exponential) are presented for elements with significant relationships with land use. I_{geo} values range from <0 (no pollution), to I_{geo} > 4 (heavy pollution). Note the different scales of each axes.

sedimentation rate in this core (0.19 cm yr^{-1}, Fig. 2) indicate the age of bottom sediments (35 cm depth) is beyond the ~150 year scope of ^{210}Pb dating (Breithaupt et al., 2018) and may predate the onset of intensified anthropogenic atmospheric Hg emissions (Cooke et al., 2010). When data from this core are excluded, mean I_{geo} in the Clarence sediments indicate no Hg contamination ($I_{geo} = -0.1 \pm 0.3$).

Although negligible pollution for most elements was observed throughout the six regional estuaries, development was often related with the degree of contamination. There were strong positive correlations between I_{geo} and development for Cd, As, Cu, Fe, and Mn (Fig. 3). Despite no significant pollution, the evident influence of development on increasing I_{geo} with respect to certain metals and metalloids demonstrates that this measure of contamination is especially sensitive to minor deviations from the geological background and may be a valuable tool to assess contamination across smaller (regional) scales. Furthermore, this study did not measure parameters required to determine ecosystem health, such as the Soil Management Assessment Framework, important in determining the quality of specific habitats (Jimenez et al., 2022).

3.3. Principal component analysis

Two principal components (PC1 and PC2) were extracted representing 36.8 and 19.5 % of the variability, respectively. Factor loadings indicate elevated sedimentation rates and increasing concentrations of elements associated with increased sedimentation (i.e. Al, Fe) (McCave, 1984), agrochemicals (P, Cd, Zn, As, Hg) (McLaughlin et al., 1996), or industrial activities (Pb, Zn, Hg Cd) (Birch et al., 1996) were strongly positively correlated with PC1. The small angles between these metals on the PCA biplot (Fig. 4) imply an association and similar source. The factor loadings of contaminants and total anthropogenic land use in the catchment (agricultural and urban land use) reflect the influence of anthropogenic development on the PCA scores of sediment samples. Therefore, we interpreted the correlation of samples with PC1 to represent the geochemical signature from anthropogenic development within the blue carbon sediments.

There was a distinct lack of PCA score grouping among samples indicating no separation between estuarine sediments across locations and land uses. However, the PCA scores showed a gradient of increasing contamination in the recent sediments of the more developed catchments. The estuaries affected by urban or agricultural development had greater concentrations of contaminants typically associated with agriculture, urbanisation, or lithogenic origin indicative of sediment deposition (i.e. P, Cu, Pb, Zn, As, Cd, Hg, Fe, and Al), as indicated by correlations between PCA scores of superficial sediments with the explanatory variables of PC1 (Fig. 4). The observations most strongly correlated with PC1 were the top ~20 cm of the Hearnes, Coffs, Boambee, and Clarence samples. Thus, the PCA revealed that the recently deposited sediments from the more developed catchments had elevated sedimentation and concentrations of metals, metalloids, and phosphorous.

While the geophysical processes governing catchment erosion and estuarine sedimentation are likely similar, catchment size (and thus fluvial transport distance necessary before deposition) and estuary morphology appear to drive sediment contaminant accumulation. The size of the catchment and estuary, in addition to less development, has likely preserved blue carbon sediment quality in the larger catchments of Corindi and Wooli. Observations from larger catchments (Wooli, Corindi, Clarence) clustered away from the smaller, more developed catchments (Fig. 4), and were strongly associated with catchment to estuary ratios (PC2) rather than the influence of development and associated lithogenic contaminant inputs (PC1).

Catchment size and estuary surface area explained elevated contaminant flux in one highly cultivated estuary of the Baltic sea, while anthropogenic land use drove increased contamination in larger catchments (Vaalgamaa and Conley, 2008). Despite similar estuary size and intense urban land uses, recent ICOLL sediments of a 7.5 km^2 catchment in nearby southeast Australia were more enriched than the adjacent 20.8 km^2 catchment (Hollins et al., 2011). Episodic catchment erosion and deposition were suggested to govern sedimentation. Our PCA results and the existing literature imply terrestrially derived contaminant mobilisation to blue carbon sediments may occur on a slower timescale in larger catchments. Comparing our results to the literature provides further evidence that these small blue carbon system still function as important filters of pollution to commercially and ecologically important marine ecosystems.

While development may accelerate sediment deposition into estuaries by 5–10 % (Dearing and Jones, 2003) and increase estuarine contaminant loads (Comeleo et al., 1996), erosion and deposition processes will naturally contribute terrestrial materials to blue carbon sediments (Meade,

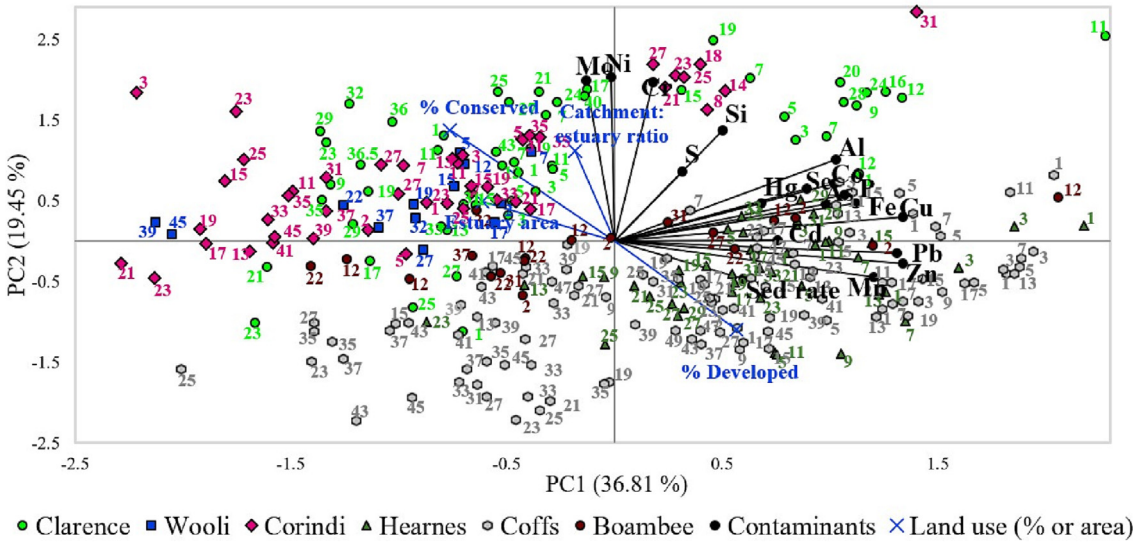

Fig. 4. Principal component (PC) and explained variabilities distance biplot of observations (sediment sample intervals, coloured dots) and explanatory variables (contaminant concentrations, black dots) or land characteristics (blue crosses). Angles between variables represent their correlation with one another. Variables with angles <90° between them are closely correlated, variables with 90° angles have no correlation, and variables with angles approaching 180° are negatively correlated. Vector length of variables represents their contributions to the principal components. Numbers next to observations represent depth of sample.

1972). Sediment deposition is most strongly focused at the upper reaches of tidal intrusion, where fluvial discharge meets the salt wedge (Yellen et al., 2017). Hence, trace metals/metalloids from less disturbed catchments may take longer to reach the lower reaches of estuaries or coastal oceans.

4. Implications

Our results demonstrate the capacity of blue carbon habitats to sequester contaminants and ultimately preserve estuarine and nearshore ocean water quality while facing increasing anthropogenic pressures (Newton et al., 2020). Multiple lines of evidence (concentrations, fluxes, and I_{geo}) converge to the conclusion that catchment land use drives blue carbon sediment accumulation of Cd, As, Fe, and Mn (Fig. 3), but not necessarily Al, Hg, Cu, or Cr. Cadmium and As are environmentally toxic (Tchounwou et al., 2012), and sediment redox conditions control the mobilisation of all of these elements to estuarine surface and groundwaters (Guo et al., 1997; Turner and Olsen, 2000). Our results showed that >30 % development in our catchments led to a > 50 % increases in Zn, As, Cu, Fe, and Mn concentrations.

Other elements had less pronounced, but environmentally significant, relationships with land use. Increasing P flux with regional development (whether agricultural or urban land use) may be a precursor to persistent estuarine eutrophication as sediments may turn from a P sink to a P source as observed elsewhere (Harris, 2001; Carpenter, 2005). Reduction of fertilizer use, sediment trapping and removal, and flocculation with inorganic particles are possible mechanisms to reduce P input into estuaries (Robb et al., 2003; Conley et al., 2009; Fox and Trefry, 2018). Cu contamination (as revealed by increasing concentrations and I_{geo}) is persistent in more developed estuaries likely driven by fungicide use or industrial activities (Conrad et al., 2017). Accelerated sediment delivery and subsequent infilling of these regional estuaries may reclaim tidal areas leading to the restriction of mangrove and saltmarsh growth, burial of seagrass, and constriction of fish habitats (Roy et al., 2001).

Catchment geomorphology was also an influence on blue carbon sediment contamination. Contaminant accumulation in sediments of large catchments and estuaries is slower than in small catchments with higher anthropogenic land use cover. In these regional coastal areas, land use conflicts are still incipient compared to larger urban areas. Thoughtful development may preserve estuarine ecosystem health until extensive and intensive development takes place (Birch et al., 2015; Liu et al., 2017). Dense urbanisation or agriculture should be avoided in small coastal catchments and established in upper catchments if blue carbon ecosystem health preservation is to be prioritised.

What will happen to these buried contaminants as other indirect anthropogenic impacts, such as climate change driven sea level rise, affect blue carbon sediments? Coarse marine sediment delivery to estuaries is expected to increase with sea level rise (Wolanski and Chappell, 1996; Boski et al., 2002). The displacement of fine-grained sediments (that more efficiently retain anthropogenic metals) by coarse (sandy) sediments may cause an observed landward migration of contaminated sediments, due to increased accumulation of sandy sediments associated with land reclamation from the current estuary mouths in a seaward direction (Niu et al., 2021). The redistribution of specific metals/metalloid/nutrient contaminants are likely to vary based on oxidation state, grain size, and suspended solid concentration within the brackish water mixing zone (Niu et al., 2021; Wang et al., 2021c).

CRediT authorship contribution statement

All authors contributed to the interpretation and writing of the MS with our main contributions being:

Stephen R. Conrad - Primary author, data compiling, lab analysis, integration of all data sets and interpretations.

Isaac R. Santos - Analysis and interpretations of data

Shane A. White - Data collection and interpretations of data.

Ceylena J. Holloway- Analysis and interpretations of data.

Dylan R. Brown - Analysis and interpretations of data

Praktan D. Wadnerkar - Data collection and interpretations of data.

Rogger E. Correa - Data collection and interpretations of data.

Rebecca L. Woodrow - Data collection and interpretations of data.

Christian J. Sanders - Senior author and project design, data compiling, lab analysis

Data availability

Data will be made available on request.

Declaration of competing interest

The authors declare the following financial interests/personal relationships which may be considered as potential competing interests: Christian

J. Sanders reports financial support was provided by Coffs Harbour City Council. Christian J. Sanders reports a relationship with Coffs Harbour City Council that includes: funding grants.

Acknowledgements

We acknowledge that this work was undertaken on the tradition country of the Gumbaynggirr and Yaegl people. We thank Samantha Hessey for her support in providing local insight.

Funding sources

This research was funded by Coffs Harbour City Council's Environmental Levy Grant Program. IRS is supported by ARC grant FT170100327 and analytical instrumentation was funed by LE140100083.

References

Alloway, B.J., 2013. Sources of heavy metals and metalloids in soils. Heavy Metals in Soils. Springer, pp. 11–50.
Alongi, D.M., McKinnon, A.D., 2005. The cycling and fate of terrestrially-derived sediments and nutrients in the coastal zone of the great barrier reef shelf. Mar. Pollut. Bull. 51, 239–252.
Álvarez-Vázquez, M.Á., Caetano, M., Álvarez-Iglesias, P., del Canto Pedrosa-García, M., Calvo, S., De Uña-Álvarez, E., Quintana, B., Vale, C., Prego, R., 2017. Natural and anthropocene fluxes of trace elements in estuarine sediments of Galician rias. Estuar. Coast. Shelf Sci. 198, 329–342.
Andrade, R., Sanders, C., Boaventura, G., Patchineelam, S., 2012. Pyritization of trace metals in mangrove sediments. Environ. Earth Sci. 67, 1757–1762.
Arias-Ortiz, A., Masqué, P., Garcia-Orellana, J., Serrano, O., Mazarrasa, I., Marbà, N., Lovelock, C.E., Lavery, P.S., Duarte, C.M., 2018. Reviews and syntheses: 210 pb-derived sediment and carbon accumulation rates in vegetated coastal ecosystems–setting the record straight. Biogeosciences 15, 6791–6818.
Baptista Neto, J.A., Peixoto, T., Smith, B.J., Mcalister, J.J., Patchineelam, S.M., Patchineelam, S.R., Fonseca, E.M., 2013. Geochronology and heavy metal flux to Guanabara Bay, Rio de Janeiro state: a preliminary study. An. Acad. Bras. Cienc. 85, 1317–1327.
Birch, G., Evenden, D., Teutsch, M., 1996. Dominance of point source in heavy metal distributions in sediments of a major Sydney estuary (Australia). Environ. Geol. 28, 169–174.
Birch, G., Lean, J., Gunns, T., 2015. Historic change in catchment land use and metal loading to Sydney estuary, Australia (1788–2010). Environ. Monit. Assess. 187, 1–15.
Boski, T., Moura, D., Veiga-Pires, C., Camacho, S., Duarte, D., Scott, D.B., Fernandes, S., 2002. Postglacial Sea-level rise and sedimentary response in the guadiana estuary, Portugal/Spain border. Sediment. Geol. 150, 103–122.
Breithaupt, J.L., Smoak, J.M., Byrne, R.H., Waters, M.N., Moyer, R.P., Sanders, C.J., 2018. Avoiding timescale bias in assessments of coastal wetland vertical change. Limnol. Oceanogr. 63, S477–S495.
Brown, D.R., Johnston, S.G., Santos, I.R., Holloway, C.J., Sanders, C.J., 2019. Significant organic carbon accumulation in two coastal acid sulfate soil wetlands. Geophys. Res. Lett. 46, 3245–3251.
Brush, G.S., 1989. Rates and patterns of estuarine sediment accumulation. Limnol. Oceanogr. 34, 1235–1246.
Carpenter, S.R., 2005. Eutrophication of aquatic ecosystems: bistability and soil phosphorus. Proc. Natl. Acad. Sci. 102, 10002–10005.
de Carvalho Gomes, F., Godoy, J.M., Godoy, M.L.D.P., Lara de Carvalho, Z., Tadeu Lopes, R., Sanchez-Cabeza, J.A., Drude de Lacerda, L., Cesar Wasserman, J., 2009. Metal concentrations, fluxes, inventories and chronologies in sediments from sepetiba and Ribeira bays: a comparative study. Mar. Pollut. Bull. 59, 123–133.
Chaudhary, M., Ahmad, N., Mashiatullah, A., Ghaffar, A., 2013. Geochemical assessment of metal concentrations in sediment core of Korangi Creek along Karachi coast, Pakistan. Environ. Monit. Assess. 185, 6677–6691.
Comeleo, R.L., Paul, J.F., August, P.V., Copeland, J., Baker, C., Hale, S.S., Latimer, R.W., 1996. Relationships between watershed stressors and sediment contamination in Chesapeake Bay estuaries. Landsc. Ecol. 11, 307–319.
Conley, D.J., Paerl, H.W., Howarth, R.W., Boesch, D.F., Seitzinger, S.P., Karl, E.K.E., Lancelot, C., Gene, E.G.E., 2009. Controlling eutrophication: nitrogen and phosphorus. Science 123, 1014–1015.
Conrad, S.R., Santos, I.R., Brown, D.R., Sanders, L.M., van Santen, M.L., Sanders, C.J., 2017. Mangrove sediments reveal records of development during the previous century (Coffs Creek estuary, Australia). Mar. Pollut. Bull. 122, 441–445.
Conrad, S., Sanders, C.J., Santos, I., White, S., 2019a. Investigating Soil Chemistry on Intensive Horticulture Sites and in Associated Dam Sediments. Southern Cross University National Marine Science Centre, Coffs Harbour, NSW.
Conrad, S.R., Santos, I.R., White, S., Sanders, C.J., 2019b. Nutrient and trace metal fluxes into estuarine sediments linked to historical and expanding agricultural activity (Hearnes Lake, Australia). Estuar. Coasts 42, 944–957.
Conrad, S.R., Santos, I.R., White, S.A., Hessey, S., Sanders, C.J., 2020. Elevated dissolved heavy metal discharge following rainfall downstream of intensive horticulture. Appl. Geochem. 113, 104490.
Cooke, C.A., Hobbs, W.O., Michelutti, N., Wolfe, A.P., 2010. Reliance on 210Pb chronology can compromise the inference of preindustrial hg flux to lake sediments. Environ. Sci. Technol. 44, 1998–2003.
Cutshall, N.H., Larsen, I.L., Olsen, C.R., 1983. Direct analysis of 210Pb in sediment samples: self-absorption corrections. Nucl. Instrum. Methods Phys. Res. 206, 309–312.
Das, B., Nordin, R., Mazumder, A., 2009. Watershed land use as a determinant of metal concentrations in freshwater systems. Environ. Geochem. Health 31, 595–607.
Davis, J.R., Koop, K., 2006. Eutrophication in australian rivers, reservoirs and estuaries–a southern hemisphere perspective on the science and its implications. Hydrobiologia 559, 23–76.
Dearing, J.A., Jones, R.T., 2003. Coupling temporal and spatial dimensions of global sediment flux through lake and marine sediment records. Glob. Planet. Chang. 39, 147–168.
DPIE, N., 2019. Catchment Boundaries of New South Wales. Department of Planning, Industry and Environment.
Duodu, G.O., Goonetilleke, A., Ayoko, G.A., 2017. Potential bioavailability assessment, source apportionment and ecological risk of heavy metals in the sediment of Brisbane River estuary, Australia. Mar. Pollut. Bull. 117, 523–531.
ELVIS, 2021. Elevation Information System - Elevation and Depth - Foundation Spatial Data. Geoscience Australia, Symonston, Australian Capital Territory, Australia.
Eyre, B., 1998. Transport, retention and transformation of material in Australian estuaries. Estuaries 21, 540–551.
Fernandes, M.C., Nayak, G.N., 2020. Depositional environment and metal distribution in mangrove sediments within middle region of tropical estuaries, Karnataka, west coast of India. Reg. Stud. Mar. Sci. 39, 101473.
Fox, A.L., Trefry, J.H., 2018. Environmental dredging to remove fine-grained, organic-rich sediments and reduce inputs of nitrogen and phosphorus to a subtropical estuary. Mar. Technol. Soc. J. 52, 42–57.
Garbarino, J.R., Kanagy, L.K., Cree, M.E., 2006. Determination of Elements in Natural-water, Biota, Sediment, and Soil Samples Using Collision/reaction Cell Inductively Coupled Plasma-mass Spectrometry. US Department of the Interior, US Geological Survey.
Guo, T., DeLaune, R., Patrick Jr., W., 1997. The influence of sediment redox chemistry on chemically active forms of arsenic, cadmium, chromium, and zinc in estuarine sediment. Environ. Int. 23, 305–316.
Harris, G.P., 2001. Biogeochemistry of nitrogen and phosphorus in Australian catchments, rivers and estuaries: effects of land use and flow regulation and comparisons with global patterns. Mar. Freshw. Res. 52, 139–149.
Harvard, U., 2007. A Summary of Error Propagation. Harvard University Press, Cambridge, MA.
Hodgkin, E., Hamilton, B., 1993. Fertilizers and eutrophication in southwestern Australia: setting the scene. Fertil. Res. 36, 95–103.
Hollins, S.E., Harrison, J.J., Jones, B.G., Zawadzki, A., Heijnis, H., Hankin, S., 2011. Reconstructing recent sedimentation in two urbanised coastal lagoons (NSW, Australia) using radioisotopes and geochemistry. J. Paleolimnol. 46, 579–596.
Ip, C.C.M., Li, X.D., Zhang, G., Farmer, J.G., Wai, O.W.H., Li, Y.S., 2004. Over one hundred years of trace metal fluxes in the sediments of the Pearl River estuary, South China. Environ. Pollut. 132, 157–172.
Irvine, I., Birch, G., 1998. Distribution of heavy metals in surficial sediments of port Jackson, Sydney, New South Wales. Aust. J. Earth Sci. 45, 297–304.
Jimenez, L.C.Z., Queiroz, H.M., Ferreira, T.O., Cherubin, M.R., 2022. Applying the Soil Management Assessment Framework (SMAF) to assess mangrove soil quality. Sustainability (Switzerland) 14.
Lee, G., Suonan, Z., Kim, S.H., Hwang, D.-W., Lee, K.-S., 2019. Heavy metal accumulation and phytoremediation potential by transplants of the seagrass Zostera marina in the polluted bay systems. Mar. Pollut. Bull. 149, 110509.
Liu, B., Hu, K., Jiang, Z., Yang, J., Luo, X., Liu, A., 2011. Distribution and enrichment of heavy metals in a sediment core from the Pearl River estuary. Environ. Earth Sci. 62, 265–275.
Liu, A., Duodu, G.O., Goonetilleke, A., Ayoko, G.A., 2017. Influence of land use configurations on river sediment pollution. Environ. Pollut. 229, 639–646.
Lovelock, C.E., Duarte, C.M., 2019. Dimensions of blue carbon and emerging perspectives. Biol. Lett. 15, 20180781.
Machado, W., Sanders, C.J., Santos, I.R., Sanders, L.M., Silva-Filho, E.V., Luiz-Silva, W., 2016. Mercury dilution by autochthonous organic matter in a fertilized mangrove wetland. Environ. Pollut. 213, 30–35.
Mackey, A., Hodgkinson, M., 1995. Concentrations and spatial distribution of trace metals in mangrove sediments from the Brisbane River, Australia. Environ. Pollut. 90, 181–186.
Macreadie, P.I., Anton, A., Raven, J.A., Beaumont, N., Connolly, R.M., Friess, D.A., Kelleway, J.J., Kennedy, H., Kuwae, T., Lavery, P.S., 2019. The future of blue carbon science. Nat. Commun. 10, 1–13.
McCave, I., 1984. Erosion, transport and deposition of fine-grained marine sediments. Geol. Soc. Lond., Spec. Publ. 15, 35–69.
McLaughlin, M.J., Tiller, K., Naidu, R., Stevens, D., 1996. The behaviour and environmental impact of contaminants in fertilizers. Soil Res. 34, 1–54.
Mcleod, E., Chmura, G.L., Bouillon, S., Salm, R., Björk, M., Duarte, C.M., Lovelock, C.E., Schlesinger, W.H., Silliman, B.R., 2011. A blueprint for blue carbon: toward an improved understanding of the role of vegetated coastal habitats in sequestering CO2. Front. Ecol. Environ. 9, 552–560.
Meade, R.H., 1972. Transport and deposition of sediments in estuaries. Geol. Soc. Am. 133, 91–120.
Miyajima, T., Hori, M., Hamaguchi, M., Shimabukuro, H., Adachi, H., Yamano, H., Nakaoka, M., 2015. Geographic variability in organic carbon stock and accumulation rate in sediments of east and southeast asian seagrass meadows. Glob. Biogeochem. Cycles 29, 397–415.
Morton, R.A., White, W.A., 1997. Characteristics of and corrections for core shortening in unconsolidated sediments. J. Coast. Res. 761–769.
Muller, G., 1969. Index of geoaccumulation in sediments of the Rhine River. GeoJournal 2, 108–118.
Nelson, P.F., Morrison, A.L., Malfroy, H.J., Cope, M., Lee, S., Hibberd, M.L., Meyer, C.P., McGregor, J., 2012. Atmospheric mercury emissions in Australia from anthropogenic, natural and recycled sources. Atmos. Environ. 62, 291–302.

Newton, A., Icely, J., Cristina, S., Perillo, G.M., Turner, R.E., Ashan, D., Cragg, S., Luo, Y., Tu, C., Li, Y., 2020. Anthropogenic, direct pressures on coastal wetlands. Front. Ecol. Evol. 8, 144.

Nicolaidou, A., Nott, J.A., 1998. Metals in sediment, seagrass and gastropods near a nickel smelter in Greece: possible interactions. Mar. Pollut. Bull. 36, 360–365.

Niu, L., Li, J., Luo, X., Fu, T., Chen, O., Yang, Q., 2021. Identification of heavy metal pollution in estuarine sediments under long-term reclamation: ecological toxicity, sources and implications for estuary management. Environ. Pollut. 290, 118126.

Rate, A.W., Robertson, A.E., Borg, A.T., 2000. Distribution of heavy metals in near-shore sediments of the Swan River estuary, Western Australia. Water Air Soil Pollut. 124, 155–168.

Robb, M., Greenop, B., Goss, Z., Douglas, G., Adeney, J., 2003. Application of phoslock TM, an innovative phosphorus binding clay, to two Western Australian waterways: preliminary findings. The Interactions Between Sediments and Water. Springer, pp. 237–243.

Robbins, J.A., Edgington, D.N., 1975. Determination of recent sedimentation rates in Lake Michigan using pb-210 and cs-137. Geochim. Cosmochim. Acta 39, 285–304.

Roy, P., Williams, R., Jones, A., Yassini, I., Gibbs, P., Coates, B., West, R., Scanes, P., Hudson, J., Nichol, S., 2001. Structure and function of south-east Australian estuaries. Estuar. Coast. Shelf Sci. 53, 351–384.

Sanders, C.J., Santos, I.R., Silva-Filho, E.V., Patchineelam, S.R., 2006. Mercury flux to estuarine sediments, derived from pb-210 and cs-137 geochronologies (Guaratuba Bay, Brazil). Mar. Pollut. Bull. 52, 1085–1089.

Sanders, C.J., Eyre, B.D., Santos, I.R., Machado, W., Luiz-Silva, W., Smoak, J.M., Breithaupt, J.L., Ketterer, M.E., Sanders, L., Marotta, H., Silva-Filho, E., 2014. Elevated rates of organic carbon, nitrogen, and phosphorus accumulation in a highly impacted mangrove wetland. Geophys. Res. Lett. 41, 2475–2480.

Sasmito, S.D., Murdiyarso, D., Friess, D.A., Kurnianto, S., 2016. Can mangroves keep pace with contemporary sea level rise? A global data review. Wetl. Ecol. Manag. 24, 263–278.

Sastre, J., Sahuquillo, A., Vidal, M., Rauret, G., 2002. Determination of cd, cu, pb and zn in environmental samples: microwave-assisted total digestion versus aqua regia and nitric acid extraction. Anal. Chim. Acta 462, 59–72.

Sholkovitz, E.R., 1978. The flocculation of dissolved fe, mn, Al, cu, NI, co and cd during estuarine mixing. Earth Planet. Sci. Lett. 41, 77–86.

Spencer, K.L., 2002. Spatial variability of metals in the inter-tidal sediments of the Medway estuary, Kent, UK. Mar. Pollut. Bull. 44, 933–944.

Tchounwou, P.B., Yedjou, C.G., Patlolla, A.K., Sutton, D.J., 2012. Heavy metal toxicity and the environment. Molecular, Clinical and Environmental Toxicology, pp. 133–164.

Teuchies, J., Vandenbruwaene, W., Carpentier, R., Bervoets, L., Temmerman, S., Wang, C., Maris, T., Cox, T.J., Van Braeckel, A., Meire, P., 2013. Estuaries as filters: the role of tidal marshes in trace metal removal. PloS one 8, e70381.

Turner, A., Olsen, Y., 2000. Chemical versus enzymatic digestion of contaminated estuarine sediment: relative importance of iron and manganese oxides in controlling trace metal bioavailability. Estuar. Coast. Shelf Sci. 51, 717–728.

Vaalgamaa, S., Conley, D.J., 2008. Detecting environmental change in estuaries: nutrient and heavy metal distributions in sediment cores in estuaries from the Gulf of Finland, Baltic Sea. Estuar. Coast. Shelf Sci. 76, 45–56.

Valette-Silver, N.J., 1993. The use of sediment cores to reconstruct historical trends in contamination of estuarine and coastal sediments. Estuaries 16, 577–588.

Wadnerkar, P.D., Santos, I.R., Looman, A., Sanders, C.J., White, S., Tucker, J.P., Holloway, C., 2019. Significant nitrate attenuation in a mangrove-fringed estuary during a flood-chase experiment. Environ. Pollut. 253, 1000–1008.

Walling, D.E., 1999. Linking land use, erosion and sediment yields in river basins. Man and River Systems. Springer, pp. 223–240.

Wang, D., Gao, S., Zhao, Y., Chatzipavlis, A., Chen, Y., Gao, J., Zhao, Y., 2021a. An eco-parametric method to derive sedimentation rates for coastal saltmarshes. Sci. Total Environ. 770, 144756.

Wang, F., Sanders, C.J., Santos, I.R., Tang, J., Schuerch, M., Kirwan, M.L., Kopp, R.E., Zhu, K., Li, X., Yuan, J., 2021b. Global blue carbon accumulation in tidal wetlands increases with climate change. Natl. Sci. Rev. 8 (9), nwaa296.

Wang, S., Vogt, R.D., Carstensen, J., Lin, Y., Feng, J., Lu, X., 2021c. Riverine flux of dissolved phosphorus to the coastal sea may be overestimated, especially in estuaries of gated rivers: implications of phosphorus adsorption/desorption on suspended sediments. Chemosphere 287 (Pt 3), 132206.

Wen, L.-S., Warnken, K.W., Santschi, P.H., 2008. The role of organic carbon, iron, and aluminium oxyhydroxides as trace metal carriers: comparison between the Trinity River and the Trinity River estuary (Galveston Bay, Texas). Mar. Chem. 112, 20–37.

Williams, T., Bubb, J., Lester, J., 1994. Metal accumulation within salt marsh environments: a review. Mar. Pollut. Bull. 28, 277–290.

Wolanski, E., Chappell, J., 1996. The response of tropical australian estuaries to a sea level rise. J. Mar. Syst. 7, 267–279.

Woodroffe, C.D., Rogers, K., McKee, K.L., Lovelock, C.E., Mendelssohn, I., Saintilan, N., 2016. Mangrove sedimentation and response to relative sea-level rise. Annu. Rev. Mar. Sci. 8, 243–266.

Yamada, N., 2015. Kinetic energy discrimination in collision/reaction cell ICP-MS: theoretical review of principles and limitations. Spectrochim. Acta B At. Spectrosc. 110, 31–44.

Yellen, B., Woodruff, J.D., Ralston, D.K., MacDonald, D.G., Jones, D.S., 2017. Salt wedge dynamics lead to enhanced sediment trapping within side embayments in high-energy estuaries. J. Geophys. Res. Oceans 122, 2226–2242.

Zhang, C., 2006. Using multivariate analyses and GIS to identify pollutants and their spatial patterns in urban soils in Galway, Ireland. Environ. Pollut. 142, 501–511.